PHYSICAL REVIEW B **99**, 020305(R) (2019)

Rapid Communications

Understanding the thermal conductivity and Lorenz number in tungsten from first principles

Yani Chen,[1,2] Jinlong Ma,[1] and Wu Li[1,*]

[1] *Institute for Advanced Study, Shenzhen University, Shenzhen 518060, China*
[2] *Key Laboratory of Optoelectronic Devices and Systems of Ministry of Education and Guangdong Province, College of Optoelectronic Engineering, Shenzhen University, Shenzhen 518060, China*

(Received 21 September 2018; published 22 January 2019)

Tungsten is known to have a Lorenz number L larger than the Sommerfeld value ($L_0 = \pi^2 k_B^2/3e^2 = 2.445 \times 10^{-8}\ \mathtt{V}^2/\mathtt{deg}^2$) by 30%. By performing fully first-principles calculations, we are able to calculate the electrical conductivity (σ) and quantify the electronic (κ_e) and the lattice (κ_{ph}) contributions to the thermal conductivity with a high accuracy. We show that the deviation of L is entirely due to κ_{ph}, and $\kappa_e/\sigma T$ agrees with L_0 within 5%. At room temperature, κ_{ph} is 46 W/m-K, one order of magnitude larger than that in other metals even with smaller atomic mass and higher Debye temperature, and likely the largest of all metals. The large κ_{ph} is ascribed to the surprisingly weak anharmonic phonon scattering. Apart from the not-strong anharmonic interatomic interaction, the weak anharmonic phonon scattering is also facilitated with the large atomic mass, leading to small thermal displacement. The interplay between the phonon-phonon and electron-phonon scatterings leads to weak temperature dependence of κ_{ph}, and signifies the importance of an accurate solution to the Boltzmann transport equation beyond the conventional relaxation time approximation. Our findings give insights into the phonon transport in metals.

DOI: 10.1103/PhysRevB.99.020305

In metals, free electrons carry both charge and heat current. As a result, the ratio of the thermal conductivity (κ) to the electrical conductivity (σ) of a metal is proportional to the temperature (T), which is termed as Wiedemann-Franz-Lorenz law (WFL). The proportionality constant L, known as the Lorenz number, is theoretically equal to the Sommerfeld value $L_0 = \pi^2 k_B^2/3e^2 = 2.445 \times 10^{-8}\ \mathtt{V}^2/\mathtt{deg}^2$. L departs considerably from L_0 at low temperatures where the mean-free paths of free electrons for the heat and charge transport are no longer the same and in poor conductors such as rare earths where the lattice (phonons) contribution to κ can no longer be considered negligible as compared to electrons [1]. Although the measured L agrees with L_0 within a few percent in many metals, L in tungsten, a moderately good conductor, is larger than L_0 by 30% at room temperature [1]. The mechanism of this exceptional Lorenz number remains a puzzle.

It was argued that the anomalous L in transition metals is due to the complexity of the band structure but not the lattice component (κ_{ph}) of thermal conductivity [2–4]. *Ab initio* calculations based on spectral function have shown that the electronic contribution (κ_{e}) agrees with the measured κ very well for a number of elemental metals such as Al, V, Nb, Ta, Mo, Pb, and Na [5,6]. Recently, direct calculations of κ_{ph} have verified that κ_{ph} is indeed negligible in common metals including Al, Ag, and Au [7]. In 2011, Wakeham *et al.* found experimentally that the ratio of the thermal and electrical Hall conductivities in the quasi-one-dimensional metallic $\mathrm{Li_{0.9}Mo_6O_{17}}$ can be orders of magnitude larger than that found in conventional bulk metals, consistent with the Luttinger liquid theory [8,9]. Recently, κ_e an order of magnitude lower than expected from WFL was found in metallic $\mathrm{VO_2}$ near its insulator-metal transition, which was explained in terms of the absence of quasiparticles in a strongly correlated electron fluid where heat and charge diffuse independently [10]. Large L was also observed in topological insulator thin films, which is related to the surface states and bipolar diffusion [11].

Knowledge of the Lorenz number is also crucial to understand transport properties in heavily doped semiconductors, which are used for many applications including thermoelectrics. Reducing κ_{ph} is a key strategy of increasing thermoelectric figure of merit. To extract κ_{ph}, one has to subtract the κ_e from the measured κ with a presumed Lorenz number, which, however, cannot be directly verified.

First-principles calculations of phonon transport for semiconductors/insulators based on Boltzmann transport equation (BTE) [12–20] or molecular dynamics [21–24] have advanced significantly in the last decade [14]. First-principles calculations of electrical transport at the mode level [25–34] have also been enabled recently with the development of techniques for electron-phonon coupling [35–40]. In this paper, we carry out first-principles calculations for the electrical and phonon transport properties of W by solving the BTE with electron-phonon coupling accurately and beyond approximations in the literature, and elucidate the origin of the deviation of the Lorenz number.

Within the framework of BTE, we discretize the Brillouin zone into Γ-centered uniform grids. The σ tensor at temperature T can be formulated as [25]

$$\sigma = \frac{2q^2}{N_{\mathbf{k}} V k_B T} \sum_{n\mathbf{k}} f_{n\mathbf{k}}^0 \left(1 - f_{n\mathbf{k}}^0\right) \mathbf{v}_{n\mathbf{k}} \otimes \mathbf{F}_{n\mathbf{k}}, \qquad (1)$$

where q is the elementary charge, k_B is the Boltzmann constant, and V is the volume of the unit cell. $f_{n\mathbf{k}}^0$, $\mathbf{v}_{n\mathbf{k}}$, and $\mathbf{F}_{n\mathbf{k}}$ are

---

[*] wu.li.phys2011@gmail.com

the equilibrium Fermi-Dirac distribution, the electron group velocity, and the mean-free displacement of the electron state denoted with band index n and wave vector $\mathbf{k}$, respectively. $N_{\mathbf{k}}$ is the number of uniformly sampled $\mathbf{k}$ points. $\mathbf{F}_{n\mathbf{k}}$ is limited by the electron-phonon coupling interaction [25] (see the Supplemental Material [41]).

The electrical thermal conductivity tensor κ_e can be obtained as [42]

$$\kappa_e = \frac{2}{N_{\mathbf{k}} V k_B T^2} \sum_{n\mathbf{k}} f^0_{n\mathbf{k}}\left(1 - f^0_{n\mathbf{k}}\right)(E_{n\mathbf{k}} - E_f)^2 \mathbf{v}_{n\mathbf{k}} \otimes \mathbf{F}_{n\mathbf{k}} - T\sigma S^2, \tag{2}$$

with

$$\sigma S = \frac{2q}{N_{\mathbf{k}} V k_B T^2} \sum_{n\mathbf{k}} f^0_{n\mathbf{k}}\left(1 - f^0_{n\mathbf{k}}\right)(E_{n\mathbf{k}} - E_f) \mathbf{v}_{n\mathbf{k}} \otimes \mathbf{F}_{n\mathbf{k}}, \tag{3}$$

where $E_{n\mathbf{k}}$ and E_f are the corresponding electronic and Fermi energy, respectively. The κ_{ph} tensor can be obtained as [14]

$$\kappa_{\mathrm{ph}} = \frac{1}{N_{\mathbf{q}} V k_B T^2} \sum_{p\mathbf{q}} n^0_{p\mathbf{q}}\left(n^0_{p\mathbf{q}} + 1\right)(\hbar\omega_{p\mathbf{q}})^2 \mathbf{v}_{p\mathbf{q}} \otimes \mathbf{F}_{p\mathbf{q}}, \tag{4}$$

where $n^0_{p\mathbf{q}}$, $\omega_{p\mathbf{q}}$, $\mathbf{v}_{p\mathbf{q}}$, and $\mathbf{F}_{p\mathbf{q}}$ are the equilibrium Bose-Einstein distribution, the phonon frequency, the phonon group velocity, and the mean-free displacement of the phonon mode denoted with branch index p and wave vector $\mathbf{q}$, respectively. $N_{\mathbf{q}}$ is the number of uniformly sampled $\mathbf{q}$ points.

$\mathbf{F}_{p\mathbf{q}}$ is limited by the isotope (iso), anharmonic phonon-phonon (ph), and electron-phonon (el) scatterings. Since each electron-phonon scattering process involves one phonon only, the linearized phonon BTE remains the same as the case without including electron-phonon scattering [14,41],

$$\mathbf{F}_{p\mathbf{q}} = \tau_{p\mathbf{q}}(\mathbf{v}_{p\mathbf{q}} + \boldsymbol{\Delta}_{p\mathbf{q}}), \tag{5}$$

except that the phonon relaxation time ($\tau_{p\mathbf{q}}$) needs to account for the electron scattering based on Matthiessen's rule:

$$\frac{1}{\tau_{p\mathbf{q}}} = \frac{1}{\tau^{\mathtt{pp}}_{p\mathbf{q}}} + \frac{1}{\tau^{\mathtt{iso}}_{p\mathbf{q}}} + \frac{1}{\tau^{\mathtt{el}}_{p\mathbf{q}}}. \tag{6}$$

$\boldsymbol{\Delta}_{p\mathbf{q}}$ is determined by the isotope and anharmonic scattering. Expressions for $\boldsymbol{\Delta}_{p\mathbf{q}}$, $1/\tau^{\mathtt{pp}}_{p\mathbf{q}}$, $1/\tau^{\mathtt{iso}}_{p\mathbf{q}}$, and $1/\tau^{\mathtt{el}}_{p\mathbf{q}}$ can be found in the Supplemental Material [41]. $\mathbf{F}_{n\mathbf{k}}$ and $\mathbf{F}_{p\mathbf{q}}$ in each corresponding linearized BTE can be solved accurately with an iterative scheme starting with the relaxation time approximation (RTA) [14,25,41].

The electron energies, phonon frequencies, and electron-phonon coupling matrix elements were calculated with the QUANTUM ESPRESSO package [43], using density functional theory and density functional perturbation theory [44]. The local density approximation for the exchange-correlation functional with Perdew-Zunger parametrization [45] and Bachelet-Hamann-Schlueter type norm-conserving pseudopotentials [46] were used for W. The EPW package [39] was employed to perform Wannier function interpolation for the electron-phonon coupling matrix with initial 8 × 8 × 8 $\mathbf{k}$ and $\mathbf{q}$ grids. Final grids as fine as 108 × 108 × 108 are required for both $\mathbf{k}$ and $\mathbf{q}$ to achieve convergence for σ and κ_e. The SHENGBTE [14] package was modified to incorporate the electron-phonon scattering and employed to calculate κ_{ph}. More details are presented in the Supplemental Material [41].The calculated σ and κ_e as a function of temperature between 200 and 500 K are plotted in Figs. 1(a) and 1(b), respectively. For comparison, the measured σ [47] and κ [1] are also plotted. The calculated σ agrees well with the experimental data, especially below the room temperature. At room temperature, the calculated value is 2.0×10^7 S/m, and the measured value ranges from 1.77 to 1.88×10^7 S/m. The discrepancy becomes larger at higher temperatures, and might be due to the temperature dependence of the phonon dispersion and band structure [48], which are, however, not considered in the calculation. Despite agreement in σ, the calculated κ_e is appreciably lower than the measured κ. The room temperature value is only 140 W/m-K, as compared to the measured 176—179 W/m-K. The calculated κ_e is almost temperature-independent, characteristic of electronic thermal conductivity. In contrast, the measured κ displays temperature dependence. As shown in Fig. 1(c). in the whole temperature range, the calculated $L_e = \kappa_e/\sigma T$ agrees with L_0 within 5% with an almost constant value of $2.34 \times 10^{-8}\ \mathrm{V}^2/\mathrm{deg}^2$. This normal behavior of L_e suggests that the abnormal value of L in tungsten is not due to the complicated nature of transition metal's band structure, as argued in Refs. [2,3].

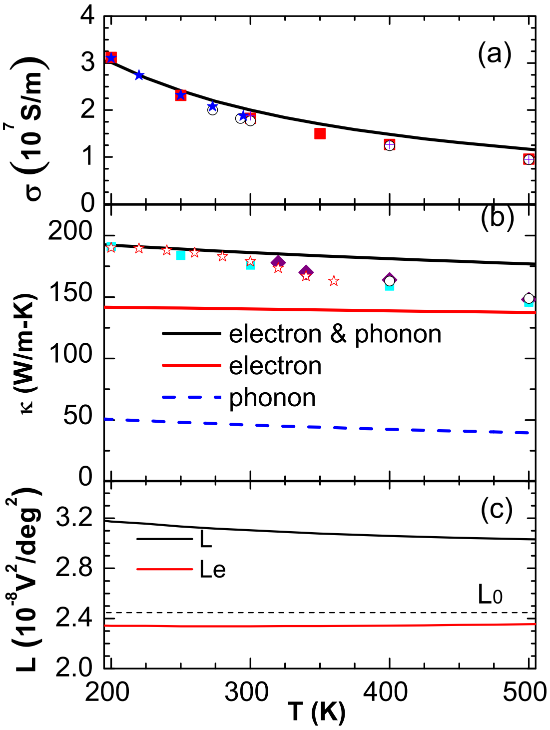

FIG. 1. (a) The electrical conductivity, (b) the thermal conductivity, and (c) the Lorenz number. The symbols show experimental electrical and thermal conductivity taken from Refs. [47] and [1], respectively.

The calculated κ_{ph} is also shown in Fig. 1(b). Surprisingly, the lattice contribution is appreciable. At room temperature, the calculated κ_{ph} is 46 W/m-K, amounting to 33% of κ_e. The calculated total thermal conductivity, $\kappa_e + \kappa_{\mathrm{ph}}$, is then 186 W/m-K, larger than the measured values only by 4–6%. The calculated total κ shows even better agreement with

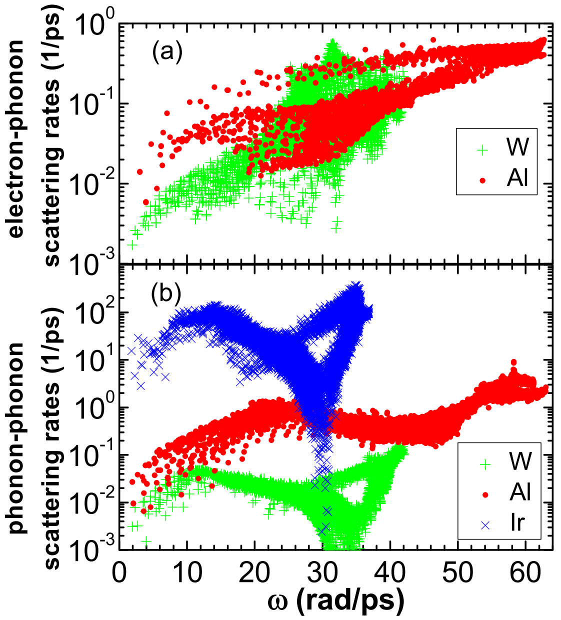

FIG. 2. Phonon scattering rates limited by (a) electron-phonon coupling for tungsten and aluminum and (b) anharmonic phonon-phonon interaction for tungsten, aluminum, and iridium at room temperature.

experiments below the room temperature, where the calculated σ also agrees with experiments better. The overestimate of calculated total κ becomes more noticeable above room temperatures, which could be mainly due to overestimated σ. ∼20% overestimate in σ at 500 K causes κ_e to be overestimated by 23 W/m-K if assuming L_e unaffected. These justify the calculated $\kappa_{\rm ph}$, and clearly indicate that the deviation of L in tungsten is due to the large lattice contribution.

$\kappa_{\rm ph}$ is about one order of magnitude larger than that in other metals. It was found that $\kappa_{\rm ph}$ at room temperature are 6, 4, and 2 W/m-K for Al, Ag, and Au, respectively [7]. To understand the much larger $\kappa_{\rm ph}$ in W, we compare the phonon scattering rates $1/\tau_{p\mathbf{q}}$ of W with Al in Fig. 2. Al is isotopically pure, and thus isotope scattering is not present. Though the isotope scattering occurs in W, it is negligible as compared to electron-phonon and phonon-phonon scatterings [41]. In Al, the anharmonic phonon-phonon scattering dominates over the electron-phonon scattering at room temperature. After neglecting the electron scattering, $\kappa_{\rm ph}$ is almost not increased in Al [7]. The anharmonic phonon-phonon scattering rates of W are almost an order of magnitude smaller than those for Al at low frequencies, and the difference is even much larger at intermediate frequencies. The electron-phonon scattering dominates over the phonon-phonon scattering at room temperature at intermediate and high frequencies in W. When excluding the electron scattering, the anharmonic scattering alone suggests a lattice thermal conductivity of 220 W/m-K, even larger than that of Si (150 W/m-K). It is, therefore, the weak anharmonic phonon scattering that leads to the large lattice thermal conductivity.

The anharmonic scattering rate is strongly correlated with the Debye temperature Θ_D [49,50]. Diamond possesses the highest thermal conductivity of all bulk systems, mainly because it has the highest Θ_D. Smaller Θ_D suggests smaller group velocities, and also usually much larger anharmonic scattering [41,50]. The more than an order of magnitude difference in $\kappa_{\rm ph}$ between Al and Si [7] can be well understood via the 50% difference in Θ_D (433 and 645 K for Al and Si, respectively) [41,51]. W has smaller Θ_D (383 K) than Al [51], which is also reflected by the smaller upper bound of the phonon frequency (Fig. 2). This relatively small difference in Θ_D is a combined consequence of the seven times larger atomic mass and few times larger harmonic (second-order) interatomic force constants (IFCs) of W. Despite smaller Θ_D, the anharmonic scattering is much weaker in W. Analysis also shows that the third-order IFCs, characterizing the anharmonicity of the interatomic potential, in W are even a few times larger than in Al [41]. Besides directly affecting the phonon frequency (Θ_D), the atomic mass also plays an important role in the anharmonic scattering [41,52]. The larger the mass, the smaller the thermal displacements, and thus the weaker the anharmonic scattering. This is reflected in the inverse mass cubed factor in the expression of transition probabilities [41]. This mass factor alone suggests two orders of magnitude smaller scattering. Further considering the stronger anharmonic interatomic interaction, the anharmonic scattering rates are eventually smaller by one order of magnitude in W.

We notice that there are several elemental metals with similar atomic mass and Θ_D such as Os, which is a poorer electrical conductor than W, and Ir with σ very close to that of W. L in these systems does not deviate from L_0 significantly [1], suggesting that $\kappa_{\rm ph}$ of these systems should be much smaller than in W. We have looked into Ir as an example. The anharmonic scattering rates in Ir are more than three orders of magnitude larger [Fig. 2(b)]. This is actually due to much stronger anharmonic IFCs in Ir [41]. The anharmonic interatomic interaction in W is neither too strong nor too weak, as compared to Ir and Al.

The interplay between the temperature-dependent phonon-phonon and temperature-independent electron-phonon scattering has two consequences. The first one is the weak temperature dependence of $\kappa_{\rm ph}$, decreasing from 50 W/m-K at 200 K only to 40 W/m-K at 500 K. This temperature dependence is much weaker than the $1/T$ dependence, which it would follow above Θ_D in the absence of electron-phonon scattering like in a semiconductor. The frequency up to which the anharmonic scattering dominates over the electron scattering increases slightly from 16 rad/ps at 200 K to 21 rad/ps at 600 K. As shown in Fig. 3, excluding electron scattering in $\kappa_{\rm ph}$ leads to a stronger variation with T.

The second consequence is the abnormal behavior of the RTA results (Fig. 3). Considering the normal processes are not resistive, RTA underestimates $\kappa_{\rm ph}$ [53]. In W, the underestimate by RTA increases significantly with temperature, which has not been observed in other systems before. $\kappa_{\rm ph}$ is underestimated by RTA by ∼50% in the absence of electron scattering, suggesting that the three-phonon processes are dominated by the normal rather than Umklapp processes [53]. The electron-phonon scattering is completely resistive. When taking the electron scattering into account, the RTA only underestimates the room temperature $\kappa_{\rm ph}$ to 39 W/m-K by 15%, as compared to the actual value of 46 W/m-K. The role of resistive electron scattering is weakened as temperature increases. Since the electron-phonon scattering is temperature

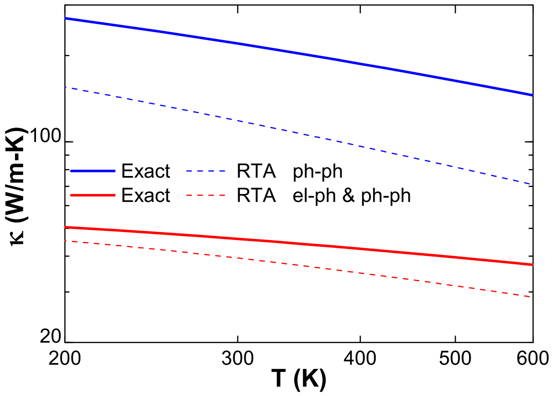

FIG. 3. The phonon thermal conductivity calculated with an exact solution (solid) and RTA (dashed) of BTE by considering only phonon-phonon scatterings and both phonon-phonon and electron-phonon scatterings.

independent, the higher the temperature, the larger the portion of the normal processes. As a result, the underestimate of the RTA increases significantly with temperature. The underestimate increases from 10% at 200 K to 23% at 600 K.

In summary, we perform first-principles calculations for the electrical and thermal conductivities of W based on the accurate solution of BTE. The results unveil that the lattice contribution to the thermal conductivity is strikingly large, as compared to other metals, leading to large deviation of the Lorenz number. The large lattice contribution is due to the weak anharmonic phonon scattering, which arises from the small thermal displacement caused by the large atomic mass in addition to the not-strong anharmonic interatomic interaction. The interplay between the temperature-independent electron-phonon and temperature-dependent phonon-phonon scattering in W results in weak temperature dependence of lattice thermal conductivity, and shows the importance of solving the BTE accurately beyond the RTA.

We acknowledge N. Mingo for helpful discussions and support from the Shenzhen Science, Technology and Innovation Commission under Grant No. JCYJ20170412105922384 and the Natural Science Foundation of China under Grants No. 11704258 and No. 11804229. Y.C. also acknowledges the support from the China Postdoctoral Science Foundation under Grant No. 2017M622745.

[1] *Landolt-Börnstein*, Group III, New Series, Vol. 15c, edited by K.-H. Hellwege and O. Madelung (Springer, Berlin, 1991).
[2] M. Cox, Phys. Rev. **64**, 241 (1943).
[3] P. Klemens, in *Thermal Conductivity*, Vol. 1, edited by R. P. Tye (Academic Press Inc., New York, 1969), p. 1.
[4] J. F. Goff, Phys. Rev. B **1**, 1351 (1970).
[5] S. Y. Savrasov and D. Y. Savrasov, Phys. Rev. B **54**, 16487 (1996).
[6] R. Bauer, A. Schmid, P. Pavone, and D. Strauch, Phys. Rev. B **57**, 11276 (1998).
[7] A. Jain and A. J. H. McGaughey, Phys. Rev. B **93**, 081206 (2016).
[8] N. Wakeham, A. F. Bangura, X. Xu, J.-F. Mercure, M. Greenblatt, and N. E. Hussey, Nat. Comm. **2**, 396 (2011).
[9] A. Garg, D. Rasch, E. Shimshoni, and A. Rosch, Phys. Rev. Lett. **103**, 096402 (2009).
[10] S. Lee, K. Hippalgaonkar, F. Yang, J. Hong, C. Ko, J. Suh, K. Liu, K. Wang, J. J. Urban, X. Zhang *et al.*, Science **355**, 371 (2017).
[11] Z. Luo, J. Tian, S. Huang, M. Srinivasan, J. Maassen, Y. P. Chen, and X. Xu, ACS Nano **12**, 1120 (2018).
[12] D. A. Broido, M. Malorny, G. Birner, N. Mingo, and D. A. Stewart, Appl. Phys. Lett. **91**, 231922 (2007).
[13] L. Lindsay, D. A. Broido, and T. L. Reinecke, Phys. Rev. Lett. **109**, 095901 (2012).
[14] W. Li, J. Carrete, N. A Katcho, and N. Mingo, Comput. Phys. Commun. **185**, 1747 (2014).
[15] L. Lindsay, D. A. Broido, and T. L. Reinecke, Phys. Rev. Lett. **111**, 025901 (2013).
[16] J. Carrete, W. Li, N. Mingo, S. Wang, and S. Curtarolo, Phys. Rev. X **4**, 011019 (2014).
[17] B. Liao, B. Qiu, J. Zhou, S. Huberman, K. Esfarjani, and G. Chen, Phys. Rev. Lett. **114**, 115901 (2015).
[18] T. Tadano, Y. Gohda, and S. Tsuneyuki, Phys. Rev. Lett. **114**, 095501 (2015).
[19] J. He, M. Amsler, Y. Xia, S. S. Naghavi, V. I. Hegde, S. Hao, S. Goedecker, V. Ozoliņš, and C. Wolverton, Phys. Rev. Lett. **117**, 046602 (2016).
[20] A. Katre, J. Carrete, B. Dongre, G. K. H. Madsen, and N. Mingo, Phys. Rev. Lett. **119**, 075902 (2017).
[21] A. Marcolongo, P. Umari, and S. Baroni, Nat. Phys. **12**, 80 (2016).
[22] C. Carbogno, R. Ramprasad, and M. Scheffler, Phys. Rev. Lett. **118**, 175901 (2017).
[23] J. Kang and L.-W. Wang, Phys. Rev. B **96**, 020302 (2017).
[24] J. S. Tse, N. J. English, K. Yin, and T. Iitaka, J. Phys. Chem. C **122**, 10682 (2018).
[25] W. Li, Phys. Rev. B **92**, 075405 (2015).
[26] B. Qiu, Z. Tian, A. Vallabhaneni, B. Liao, J. M. Mendoza, O. D. Restrepo, X. Ruan, and G. Chen, Europhys. Lett. **109**, 57006 (2015).
[27] M. Fiorentini and N. Bonini, Phys. Rev. B **94**, 085204 (2016).
[28] J.-J. Zhou and M. Bernardi, Phys. Rev. B **94**, 201201(R) (2016).
[29] T.-H. Liu, J. Zhou, B. Liao, D. J. Singh, and G. Chen, Phys. Rev. B **95**, 075206 (2017).
[30] T.-H. Liu, J. Zhou, M. Li, Z. Ding, Q. Song, B. Liao, L. Fu, and G. Chen, Proc. Natl. Acad. Sci. USA **115**, 879 (2018).
[31] J. Ma, A. S. Nissimagoudar, and W. Li, Phys. Rev. B **97**, 045201 (2018).
[32] J. Ma, Y. Chen, and W. Li, Phys. Rev. B **97**, 205207 (2018).
[33] S. Poncé, E. R. Margine, and F. Giustino, Phys. Rev. B **97**, 121201 (2018).
[34] T.-H. Liu, B. Song, L. Meroueh, Z. Ding, Q. Song, J. Zhou, M. Li, and G. Chen, Phys. Rev. B **98**, 081203 (2018).
[35] F. Giustino, M. L. Cohen, and S. G. Louie, Phys. Rev. B **76**, 165108 (2007).

[36] K. Kaasbjerg, K. S. Thygesen, and K. W. Jacobsen, Phys. Rev. B **85**, 115317 (2012).

[37] J. Sjakste, N. Vast, M. Calandra, and F. Mauri, Phys. Rev. B **92**, 054307 (2015).

[38] C. Verdi and F. Giustino, Phys. Rev. Lett. **115**, 176401 (2015).

[39] S. Poncé, E. Margine, C. Verdi, and F. Giustino, Comput. Phys. Commun. **209**, 116 (2016).

[40] F. Giustino, Rev. Mod. Phys. **89**, 015003 (2017).

[41] See Supplemental Material at http://link.aps.org/supplemental/10.1103/PhysRevB.99.020305 for more details on the methodology, the isotope scattering rates of W, the analysis of the anharmonic scattering, and phonon dispersions, and the anharmonic interatomic force constants of W, Al, and Ir, which includes Refs. [54–56].

[42] G. K. Madsen and D. J. Singh, Comput. Phys. Commun. **175**, 67 (2006).

[43] P. Giannozzi, S. Baroni, N. Bonini, M. Calandra, R. Car, C. Cavazzoni, D. Ceresoli, G. L. Chiarotti, M. Cococcioni, I. Dabo, A. D. Corso, S. de Gironcoli, S. Fabris, G. Fratesi, R. Gebauer, U. Gerstmann, C. Gougoussis, A. Kokalj, M. Lazzeri, L. Martin-Samos, N. Marzari, F. Mauri, R. Mazzarello, S. Paolini, A. Pasquarello, L. Paulatto, C. Sbraccia, S. Scandolo, G. Sclauzero, A. P. Seitsonen, A. Smogunov, P. Umari, and R. M. Wentzcovitch, J. Phys.: Condens. Matter **21**, 395502 (2009).

[44] S. Baroni, S. de Gironcoli, A. Dal Corso, and P. Giannozzi, Rev. Mod. Phys. **73**, 515 (2001).

[45] J. P. Perdew and A. Zunger, Phys. Rev. B **23**, 5048 (1981).

[46] G. B. Bachelet, D. R. Hamann, and M. Schlüter, Phys. Rev. B **26**, 4199 (1982).

[47] *Landolt-Börnstein*, Group III, New Series, Vol. 15a, edited by K.-H. Hellwege and O. Madelung (Springer, Berlin, 1982).

[48] J. M. Ziman, *Electrons and Phonons: The Theory of Transport Phenomena in Solids* (Clarendon Press, London, 1960).

[49] G. Leibfried and E. Schlömann, Nachr. Akad. Wiss. Göttingen, Math. Phys. Klasse **4**, 71 (1954).

[50] W. Li and N. Mingo, Phys. Rev. B **89**, 184304 (2014).

[51] A. Tari, *The Specific Heat of Matter at Low Temperatures* (Imperial College Press, London, 2003).

[52] W. Li and N. Mingo, Phys. Rev. B **90**, 094302 (2014).

[53] A. Ward, D. A. Broido, D. A. Stewart, and G. Deinzer, Phys. Rev. B **80**, 125203 (2009).

[54] A. Larose and B. N. Brockhouse, Can. J. Phys. **54**, 1819 (1976).

[55] R. Stedman and G. Nilsson, Phys. Rev. **145**, 492 (1966).

[56] R. Heid, K.-P. Bohnen, K. Felix, K. M. Ho, and W. Reichardt, J. Phys.: Condens. Matter **10**, 7967 (1998).